Astronomy
&
Astrophysics

X-ray observations of the Crab Pulsar and Nebula with JEM–X on INTEGRAL[⋆]

S. Brandt[1], C. Budtz-Jørgensen[1], N. Lund[1], I. L. Rasmussen[1], S. Laursen[1], J. Chenevez[1],
N. J. Westergaard[1], G. Juchnikowski[2], R. Walter[3], M. Schmidt[4], and R. Much[5]

[1] Danish Space Research Institute, Juliane Maries Vej 30, 2100 Copenhagen Ø, Denmark
[2] Space Research Center, Bartycka 18A 00-716, Warsaw, Poland
[3] INTEGRAL Science Data Center, Chemin d'Écogia 16, Versoix, Switzerland
[4] ESOC, Robert-Bosch Str. 5, 64293 Darmstadt, Germany
[5] ESTEC, Keplerlaan 1, Postbus 299, 2200 AG Noordwijk, The Netherlands

Abstract. The Crab pulsar is the best studied rotation powered pulsar. We report the results obtained in the 3–35 keV energy band with the X-ray monitor, JEM–X, on ESAs recently launched γ-ray mission, INTEGRAL.

Key words. pulsars: individual: PSR B0531+21 – X-rays: stars – instrumentation: detectors

1. Introduction

The Crab pulsar, with a 33 ms period, has been studied by many X-ray missions with timing capabilities since the first reports in the late 1960's (Fritz et al. 1969). The INTEGRAL mission (Winkler et al. 2003), in addition to the main γ-ray instruments, also carries an X-ray monitor, JEM–X. The JEM–X monitor consists of two identical, independent X-ray detectors with coded masks, covering the energy range of 3–35 keV (Lund et al. 2003). Each detector has a sensitive area of $\approx$330 cm^2 and a field of view of 6.6°. The time resolution for X-ray events in the normal observation mode is 122 μs (Brandt et al. 2003).

2. Observations

The Crab Nebula was observed by INTEGRAL in February 2003, as part of the instrument calibration campaign. The observations used in this study are listed in Table 1. The total set of observations include 5.5×10^6 photons in the pulsed fraction of the Pulsar over the constant signal from the Nebula and the background of 60×10^6 events. For on-axis observations, which constitute most of the included data, the pulsed fraction contributes 9%, the Nebula 76%, and 4% of the counts are cosmic diffuse X-rays, finally about 11% of the counts derive from particle interactions (Brandt et al. 2003). In order to maintain a good signal to noise ratio, only observations with the Crab closer than 3° from the center of the field of view, corresponding to better than 70% of the on-axis sensitivity, were used. For some of the observations the telemetry bandwidth did not allow the transmission of all data, but the automatic grey-filter mechanism (Brandt et al. 2003) used to reduce the data rate does not affect the timing studies, as the pulsar period is much shorter than the timescale of any grey-filter changes.

3. Absolute timing

The Crab Pulsar is useful for the purpose of verifying the absolute timing of the JEM–X instrument and the INTEGRAL ground segment.

The most accurate and reliable determination of the relation between the arrival phases of the main pulses in the radio and the X-ray band is believed to be that of the Rossi-XTE mission (determined by Rots, referenced in Tennant et al. 2001) with the X-ray peak leading the radio peak by 300 ± 67 μs, corresponding to 0.009 ± 0.002 in phase.

The arrival times of the photons corrected to the Solar System barycenter were folded using the period derived from the monthly radio ephemeris of Jodrell Bank (Lyne et al. 2003). The JPL DE200 planetary ephemeris are used with IDL routines developed by E. Goehler and C. Marquardt.

The JEM–X timing relative to the INTEGRAL onboard clock was measured during ground calibrations. The JEM–X time tagging was found to lag the onboard time by 183 μs (Brandt et al. 2003, and references therein; Lund 2002).

Prompted by the initial analysis of the data from JEM–X, an error was found in the ground segment time relation software by the INTEGRAL Mission Operations Center.

Table 1. Summary of the Crab observations used in this work. In some cases the observations were limited by the telemetry allocation and the onboard grey filter mechanism applied. Only pointings with the Crab closer than 3° from the center of the field of view have been used. The constant term includes the instrumental background, the diffuse X-ray background, and the Crab Nebula itself. The epoch of INTEGRAL Julian Day has an origin at Jan. 01, 2000 (Walter et al. 2003).

Integral Julian Day	Date	Duration ks	Orbit	Pointing IDs	JEM–X1 pulsed ($\times 10^3$)	JEM–X1 constant ($\times 10^3$)	JEM–X2 pulsed ($\times 10^3$)	JEM–X2 constant ($\times 10^3$)	Spacecraft Mode
1133.89	07 Feb. 2003	96	39	2	174	1840	182	1835	staring
1135.37	09 Feb. 2003	69	39	5	503	5651	546	5604	staring
1136.93	10 Feb. 2003	124	40	2–4	904	10 033	972	9992	staring
1143.01	17 Feb. 2003	64	42	7–14	414	4777	524	5515	scan
1144.09	18 Feb. 2003	33	42	18	99	1024	143	1432	staring
1146.04	20 Feb. 2003	54	43	5–32	182	2150	262	2886	hex dither
1147.15	21 Feb. 2003	34	43	40–79	112	1454	165	1950	5×5 dither
1149.01	23 Feb. 2003	40	44	8–63	137	1712	205	2302	5×5 dither

Table 2. The various timing offsets applied for the epoch of this study to correct the time relation delivered by the Integral Science Data Center (ISDC).

Source	Offset μs (to be added)
JEM–X internal	183
Operations Center Software	964
Redu Ground Station	−103
Goldstone DSS-16 Ground Station	42

The error requires 964 μs to be added to the derived absolute time (Walter et al. 2003). This part of the software is shared with the XMM mission, and the offset is also applicable to the XMM data. This may bring the derived arrival time of the Crab X-rays relative to the radio peak reported from XMM (Becker & Aschenbach 2002) in better agreement with our results derived below.

The INTEGRAL mission uses two ground stations during its orbit (Much et al. 2003). The primary station is the ESA station in Redu and the secondary is NASA's Goldstone station. For the epoch of the observations presented here, there is a discrepancy of 145 μs in the time relation derived by the two stations (Walter et al. 2003; Schmidt 2003). The corrections used are listed in Table 2.

The total pulse profile is shown in Fig. 1. The phase is relative to the arrival time of the main radio peak. The pulse profile has the familiar shape of a main and secondary peak separated by 0.4 in phase, and connected by a "bridge" of emission. The pulse profile is well fitted with a set of five exponential wavelets, as noted by Tennant et al. (2001). Two wavelets each describe the rise and fall of the main and secondary peak. The fifth wavelet describes the bridge, starting at the main peak. The wavelets are a useful tool to quantify the change of the pulse profile as a function of energy. The position of the peaks in phase are defined as the intersection of the fitted wavelets.

As expected, it is found that the X-ray peak is leading the radio peak. The determined lead of the X-ray peak relative to the radio is shown in Fig. 2. The lead is determined for
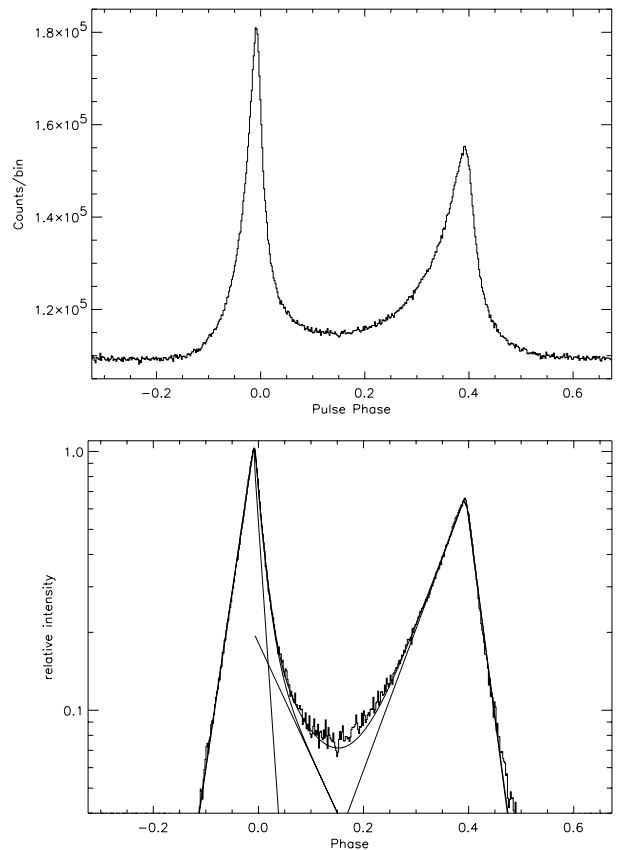
Fig. 1. The Crab pulse profile derived from the observation in Table 1 over the total JEM–X energy range (3.5–35 keV). The pulsed fraction contains 5.6×10^6 events over the Nebula and background of 60×10^6 events. The data are folded in 550 bins, corresponding to ≈61 μs. The lower panel shows the pulsed fraction on a log scale. The solid line a is fit of simple exponential wavelets, whose components are also indicated.

each observation listed in Table 1. The pulse profiles for the two JEM–X instruments have been combined, as it is found by this analysis that any remaining timing offsets are identical for the two units. The weighted averages for the separate observations give 338 μs for JEM–X1, and 337 μs for JEM–X2.
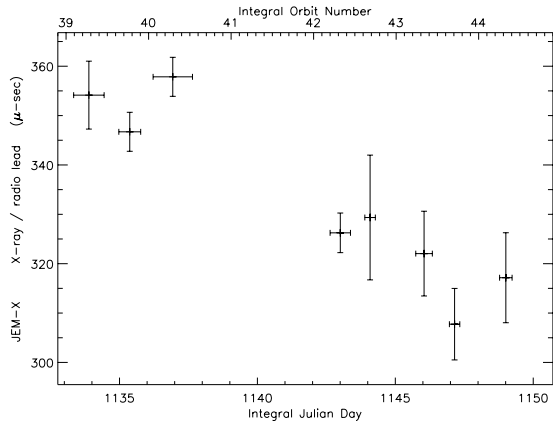
Fig. 2. The derived lead of the Crab pulsar main peak in the 3–35 keV X-ray band relative to the arrival of the radio peak derived for each of the eight observations in Table 1.
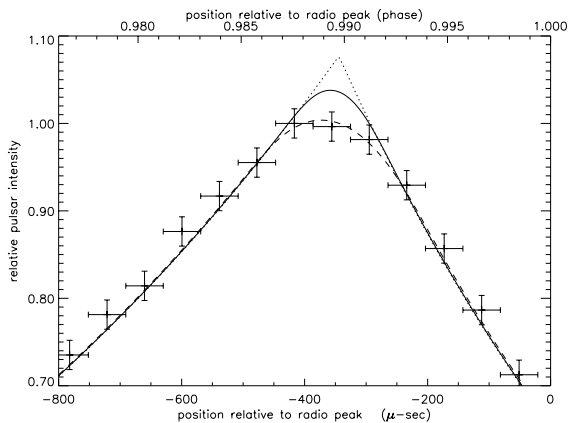
Fig. 3. Detail around the main peak of the Crab pulse profile for the total set of observations. The data are binned with $61\,\mu$s resolution. The error bars reflect the counting statistics. The solid line is the best fit of two exponentials in a 2 ms interval with a smoothing of $122\,\mu$s and $61\,\mu$s. The dotted line is the two exponentials and the dashed line is smoothed with $250\,\mu$s.

The results for the 8 observations scattered over a 17 day period fall within a range of $60\,\mu$s. The lead determined from one co-added pulse profile, shown in Fig. 1 and in detail in Fig. 3, is $335\,\mu$s with a statistical uncertainty of $5\,\mu$s. The uncertainties introduced by systematics, other sources of uncertainties, and possible intrinsic variability of the X-ray lead are harder to estimate. The scatter of $\pm30\,\mu$s of the points derived from each separate observation, may be taken as an indicator of the stability of the combined timing system of JEM–X and INTEGRAL. Some systematic errors in the absolute pulse phase may be introduced in the extrapolation of the radio ephemeris. Allowing room for systematics, a conservative estimate for the lead is $335 \pm 100\,\mu$s, or a position in phase of 0.990 ± 0.003, consistent with other studies of the INTEGRAL data (Kuiper et al. 2003).

4. Spectral properties

The spectral properties of the Crab Pulsar over a wide energy range have been studied in detail (Kuiper et al. 2001).
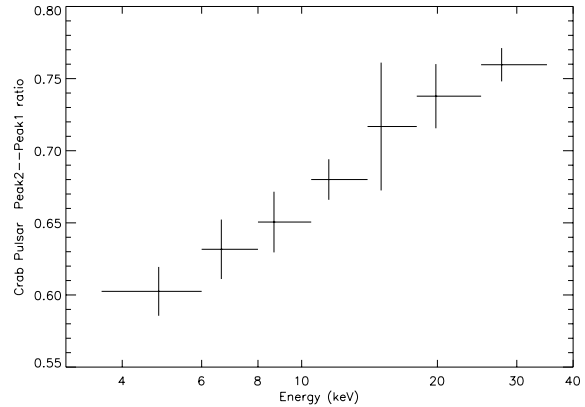
Fig. 4. The intensity of the Crab pulsar main peak relative to the secondary peak as a function of energy.
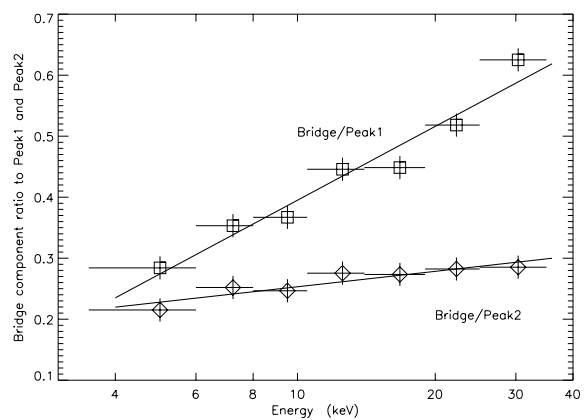
Fig. 5. The flux of the fitted bridge component relative to the flux of the main peak (Peak1) and the secondary peak (Peak2) as a function of energy.

The development of the pulse shape, as a function of energy may be described by the parameters of the wavelets shown in Fig. 1. Here we will only comment on a couple of these features.

The ratio of the secondary to the main peak of the pulse is increasing with energy in the X-ray range. The result in the JEM–X range of 3–35 keV is shown in Fig. 4, where we see that the ratio of the second peak to the main peak increases from $\approx$0.60 at 5 keV to $\approx$0.75 at 30 keV.

The bridge component is increasing in intensity relative to the intensity of the main peak and the secondary peak, as a function of energy. These ratios are shown in Fig. 5.

5. Relative position of the Nebula and the Pulsar

The Crab Nebula has an extent, measured as half-width, of the order of 1′ in the X-ray range. Our observations may be used to study the over-all spatial relation of the Nebula relative to the Pulsar in the energy range 3–25 keV, and to demonstrate the positioning capabilities of JEM–X. The resolution of 3.4′ of JEM–X (Lund et al. 2003) does not allow a mapping of the Nebula like the high resolution X-ray missions of Chandra (Weiskopf et al. 2000) and XMM-Newton (Willingale 2001). However, the data binned according to pulse phase allows the
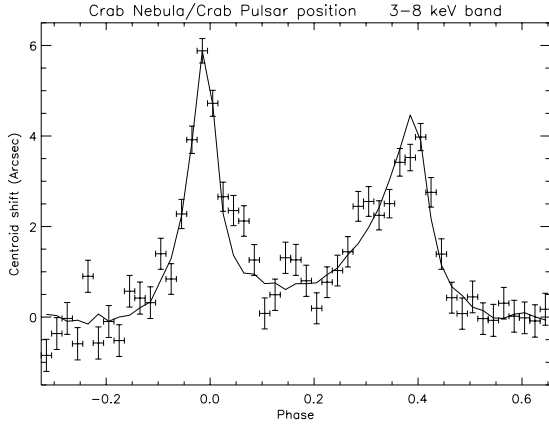
Fig. 6. The displacement of the centroid of the Nebula-Pulsar complex as a function of pulse phase in the 3–8 keV range. The 5.9″ amplitude corresponds to an offset between the Pulsar and the Nebula centroid of 14.4″ ± 1.4″. The solid line is based on the relative intensity of the pulsed fraction and the constant contribution from the Nebula. The displacement is positive in the S–E direction.

Table 3. The offset of the pulsed fraction of the Crab relative to the centroid of the Nebula as a function of energy.

Energy (keV)	Offset (arcsec)
3–8	14.4 ± 1.4
8–13	12.7 ± 1.3
13–25	10.5 ± 1.0

determination of the relative positions of the pulsar and the centroid of the Nebula (Pelling et al. 1987). We assume the unpulsed fraction of the Pulsar flux to be negligible.

The analysis was performed using data from orbit 40 (Table 1). The data were divided into 3 energy bands, each with 50 pulsar phase bins. The offset, Δ, between the Pulsar and the diffuse Nebula is found by fitting the determined offset as a function of phase to the functional shape determined by the ratio of the pulsed (I_{pulsed}) and the total signal ($I_{\mathrm{DC}} + I_{\mathrm{pulsed}}$) from the Crab complex:

$$\Delta_{\mathrm{Obs}} \quad = \quad \Delta \quad \times \quad \frac{I_{\mathrm{pulsed}}}{I_{\mathrm{DC}} + I_{\mathrm{pulsed}}}. \tag{1}$$

The two JEM–X units are mounted with a 180° relative rotation, thus the effect is in opposite directions in the local coordinate systems. The combined results are summarized in Table 3. The determined angular offset as a function of pulse phase for the 3–8 keV energy band is shown in Fig. 6. We see that the offset in position is slightly decreasing as a function of energy. The statistical uncertainty for each determined position, as a function of phase, is ≈0.34″ and the standard deviation from the best fitting curve is 0.5″. The centroid of the Nebula is

found to be displaced from the Pulsar in the N–W direction, as expected (Pelling et al. 1987; Weiskopf et al. 2000).

6. Conclusions

We determined the lead of the Crab X-ray pulse relative to the radio pulse and found a value of 335 ± 100 μs. This is consistent with other observations and confirms the stability of the INTEGRAL and JEM–X timing systems to within ±30 μs. The absolute timing is found to be accurate to the level of ±100 μs.

The analysis of the displacement of the Nebula centroid relative to the Pulsar demonstrates that the relative position determination with JEM–X is close to the statistical limit, promising absolute positions with arcsecond accuracy, once systematic effects are properly understood.

References

Brandt, S., Budtz-Jørgensen, C., Lund, N., et al. 2003, A&A, 411, L243

Becker, W., & Aschenbach, B. 2002, X-ray Observations of Neutron Stars and Pulsars: First Results from XMM-Newton, in Neutron Stars and Supernova Remnants, ed. W. Becker, H. Lesch, & J. Trümper, MPE Report, 278, 64

Fritz, G., Henry, R. C., Meekins, J. F., et al. 1969, Science, 164, 709

Kuiper, L., Hermsen, W., Walter, R., & Foschini, L. 2003, A&A, 411, L31

Kuiper, L., Hermsen, W., Cusumano, G., et al. 2001, A&A, 378, 918

Lund, N. 2002, Joint European X-Ray Monitor JEM–X, User Manual, Issue 5.5, October 10, 2002, `www.dsri.dk`

Lund, N., Budtz-Jørgensen, C., Westergaard, N. J., et al. 2003, A&A, 411, L231

Lyne, A. G., Jordan, C. A., & Roberts, M. E. 2003, Jodrell Bank Crab Pulsar Timing Results, Monthly Ephemeris, University of Manchester

Much, R., Barr, P., Hansson, L., et al. 2003, A&A, 411, L49

Pelling, R. M., Paciesas, W. S., Peterson, L. E., et al. 1987, ApJ, 319, 416

Schmidt, M. 2003, INTEGRAL Mission Operations Center, Private communication

Tennant, A. F., Becker, W., Juda, M., et al. 2001, ApJ, 554, L173

Walter, R., Favre, P., Dubath, P., et al. 2003, A&A, 411, L25

Weisskopf, M. C., Hester, J. J., Tennant, A. F., et al. 2000, ApJ, 536, L81

Willingale, R., Aschenbach, B., Griffiths, R. G., et al. 2001, A&A, 365, L212

Winkler, C., Courvoisier, T. J.-L., Di Cocco, G., et al. 2003, A&A, 411, L1